JACS
JOURNAL OF THE AMERICAN CHEMICAL SOCIETY

ARTICLE

pubs.acs.org/JACS

Dinuclear Zn(II) Complex Catalyzed Phosphodiester Cleavage Proceeds via a Concerted Mechanism: A Density Functional Theory Study

Hui Gao,[†] Zhuofeng Ke,[†] Nathan J. DeYonker,[‡] Juping Wang,[†] Huiying Xu,[†] Zong-Wan Mao,[†] David Lee Phillips,[*,§] and Cunyuan Zhao[*,†]

[†]MOE Key Laboratory of Bioinorganic and Synthetic Chemistry/KLGHEI of Environment and Energy Chemistry, School of Chemistry and Chemical Engineering, Sun Yat-Sen University, Guangzhou 510275, P. R. China

[‡]Department of Chemistry, The University of Memphis, Memphis, Tennessee 38152-3550, United States

[§]Department of Chemistry, The University of Hong Kong, Pokfulam Road, Hong Kong, P. R. China

Supporting Information

ABSTRACT: Density functional theory (DFT) calculations were used to study the mechanism for the cleavage reaction of the RNA analogue **HpPNP** (**HpPNP** = 2-hydroxypropyl-4-nitrophenyl phosphate) catalyzed by the dinuclear Zn(II) complex of 1,3-bis(1,4,7-triazacyclonon-1-yl)-2-hydroxypropane ($\mathbf{Zn_2(L_2O)}$). We present a binding mode in which each terminal phosphoryl oxygen atom binds to one zinc center, respectively, and the nucleophilic 2-hydroxypropyl group coordinates to one of the zinc ions, while the hydroxide from deprotonation of a water molecule coordinates to the other zinc ion. Our calculations found a concerted mechanism for the **HpPNP** cleavage with a 16.5 kcal/mol reaction barrier. An alternative proposed stepwise mechanism through a pentavalent oxyphosphorane dianion reaction intermediate for the **HpPNP** cleavage was found to be less feasible with a significantly higher energy barrier. In this stepwise mechanism, the deprotonation of the nucleophilic 2-hydroxypropyl group is accompanied with nucleophilic attack in the rate-determining step. Calculations of the nucleophile ^{18}O kinetic isotope effect (KIE) and leaving ^{18}O KIE for the concerted mechanism are in reasonably good agreement with the experimental values. Our results indicate a specific-base catalysis mechanism takes place in which the deprotonation of the nucleophilic 2-hydroxypropyl group occurs in a pre-equilibrium step followed by a nucleophilic attack on the phosphorus center. Detailed comparison of the geometric and electronic structure for the **HpPNP** cleavage reaction mechanisms in the presence/absence of catalyst revealed that the catalyst significantly altered the determining-step transition state to become far more associative or tight, that is, bond formation to the nucleophile was remarkably more advanced than leaving group bond fission in the catalyzed mechanism. Our results are consistent with and provide a reliable interpretation for the experimental observations that suggest the reaction occurs by a concerted mechanism (see Humphry, T.; Iyer, S.; Iranzo, O.; Morrow, J. R.; Richard, J. P.; Paneth, P.; Hengge, A. C. *J. Am. Chem. Soc.* **2008**, *130*, 17858−17866) and has a specific-base catalysis character (see Yang, M.-Y.; Iranzo, O.; Richard, J. P.; Morrow, J. R. *J. Am. Chem. Soc.* **2005**, *127*, 1064−1065).

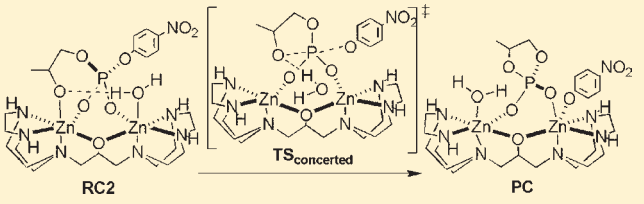

INTRODUCTION

The phosphodiester moiety plays an important role in living systems since it is a component of the backbone of DNA and RNA.[1−7] Some metal-complexes, especially zinc-containing ones, can interact with phosphodiesters to influence the chemical properties and function of the nearby nucleic acid component(s).[8−11] Much work has been devoted to the development of synthetic metal-complexes for the cleavage of DNA or RNA in order to move toward potential application as useful replacements to nucleases as laboratory tools.[12−26]

Knowledge gained from the investigation of the mechanism for metal-complex-promoted phosphodiesters cleavage reaction will help in the design of more efficient metal-complexes and also provide important insight into enzyme catalysis reactions.[27] Unfortunately, due to the lack of direct evidence for the binding mode of the substrate-catalyst complexes, uncertainty remains about the interactions of phosphodiesters and metal-complex for experimental scientists.[28] It is urgent and necessary to use computational tools to reveal the binding mode of the substrate-catalyst complex and provide more detailed information for better understanding the mechanism such as the nature of the structures of the transition states along the reaction pathway and whether the reaction takes place via a concerted or a stepwise mechanism.

There has been much discussion in the literature about the mechanism of the cleavage reaction of phosphodiester promoted by metal-complexes, with a general-base-catalyzed (GBC) pathway

Received: July 29, 2010
Published: February 14, 2011

dx.doi.org/10.1021/ja106456u | *J. Am. Chem. Soc.* 2011, 133, 2904–2915

Scheme 1. Reaction Catalyzed by Dinuclear Zn(II) Complex of $Zn_2(L_2O)$ with HpPNP as Substrate

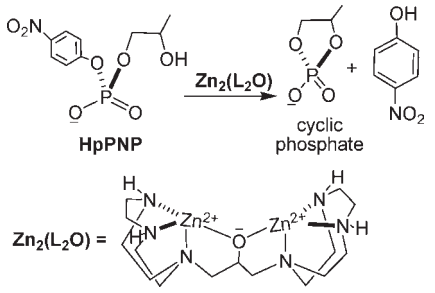

mechanism and a specific-base-catalyzed (SBC) pathway mechanism both being proposed to describe the reactions.[29−32] Recently, a mononuclear Zn(II) complex has been reported to promote the cleavage of 2-hydroxypropyl-4-nitrophenyl phosphate (**HpPNP**, a model for RNA linkage) by Williams and co-workers[33] who proposed a specific base catalysis mechanism. A density functional study on the same reaction by Fan and Gao suggested a different general-base-catalyzed mechanism.[34]

A number of metalloenzymes that catalyze the cleavage of phosphodiesters contain two metal ions in the active site, and these dinuclear complexes are often more effective and reactive than their corresponding mononuclear complexes.[35−40] Dinuclear zinc catalysts have also been found to be more effective and reactive than their corresponding mononuclear complexes for some cyclopropanation reactions with alkene substrates.[41] Therefore, it is very interesting and challenging to better understand the mechanism for the dizinc-mediated phosphodiester cleavage reaction. Recently, Richard and co-workers investigated a dinuclear zinc catalysts of 1,3-bis(1,4,7-triazacyclonon-1-yl)-2-hydroxypropane ($\mathbf{Zn_2(L_2O)}$)[42] to promote the transesterification of **HpPNP** (Scheme 1),[28,43,44] and some details of the reaction mechanism remain unclear. Subsequently, Fan and Gao proposed a possible mechanism,[45] which appears to be significantly different from the experimental observation for these reactions.[28,43,44] Herein, we attempt to gain a more detailed understanding of the catalytic mechanism by employing DFT calculations to examine the following aspects of the reaction: how the substrate and the catalyst bind to a complex, how the catalyst promotes the cleavage of **HpPNP**, how the catalyst affects the geometry of the transition states compared to the uncatalyzed reaction, how the Zn(II) ions' coordination numbers change during the reaction, what the true active forms of the catalyst are likely to be, whether the reaction takes place by a concerted or a stepwise mechanism, and whether the reaction occurs by a specific or general base catalysis mechanism.

COMPUTATIONAL DETAILS

The theoretical calculations were performed using the Gaussian 03 program,[46] and all of the reported structures were fully optimized with the density functional theory (DFT) method using the hybrid B3LYP density functional.[47,48] The Stuttgart/Dresden (SDD) with the effective core potential (ECP)[49] basis sets were used for the zinc atoms, and the 6-31G(d, p) basis sets were used for C, N, O, P, and H atoms. Natural bond orbital (NBO) analysis[50,51] was performed at the same level of theory as the one used for geometry optimizations. Frequency analyses were done in order to ensure that the optimized structures were at either a minimum or transition state. The thermodynamic functions, including the enthalpies and free energies, were calculated at 298.15 K and 1 atm. The intrinsic reaction coordinate (IRC) method[52] was performed to confirm the transition states found connected relevant reactants and products. The solvation energies for all of the species in aqueous solution were estimated by employing the polarizable continuum model (PCM)[53] with UAHF sets of radii. Recent experiments performed to characterize the mechanism have investigated the kinetic or equilibrium isotope effect (KIE or EIE) in order to probe the extent of nucleophile bond formation, leaving group bond cleavage, and charge development in the transition state.[28,54,55] In this study, we also compared the results from calculations of the nucleophile ^{18}O KIE (or EIE) and leaving ^{18}O KIE for the concerted mechanism to the experimental results. Kinetic and equilibrium isotope effects on the concerted mechanism for cleavage of **HpPNP** promoted by dinuclear Zn(II) complex were calculated within the harmonic oscillator/rigid rotor approximations, as implemented in the Gaussian 03 program.[46,56] To test the reliability of the different functionals and basis-sets, we have also calculated and compared the key structures and the reaction barriers for the concerted and stepwise pathways using the B3LYP, the BHandHLYP,[48,57] and the Tao-Perdew-Dtaroverov-Scuseria (TPSS)[58] functionals with the 6-31G(d, p)(SDD for Zn) basis sets for the geometry and frequency calculations followed by single point energy refinement with the 6-311++G-(d, p)(SDD for Zn) basis sets, respectively. The calculated reaction barriers are qualitatively similar to each other (within a few kcal/mol) with the three different methods, while the reaction barriers determined using the B3LYP and BHandHLYP gave the better agreement with experimental results than those obtained using the TPSS functional. Therefore, throughout the paper, we used the most popular functional B3LYP at the 6-31G(d, p)(SDD for Zn) level of theory as a reasonable compromise to make the computations more tractable (except for the special annotations as indicated in the text).

RESULTS AND DISCUSSION

The structure and properties of the active form of the catalyst have been actively debated for a number of years.[33,34,43a,44a] Previous experimental work determined that the complex between **HpPNP** and the fully protonated catalysts is inactive and converted to an active form upon the loss of a proton even if under neutral pH condition.[43a] There are mainly two proposed active forms for the catalyst involving two proposed mechanisms for metal-complex-promoted **HpPNP** cleavage reaction: one possibility is that the active catalyst is $\mathbf{Zn_2(L_2O)(HO^-)}$, and this is protonated to give the inactive catalyst $\mathbf{Zn_2(L_2O)(H_2O)}$. In this case, the active catalyst $\mathbf{Zn_2(L_2O)(HO^-)}$ is specific for cleavage of **HpPNP**, and the relevant proposed pathway involves deprotonation of the substrate 2-hydroxypropyl group by a zinc-bound hydroxide, which acts as general base catalyst. A second possibility is that the active catalyst is $\mathbf{Zn_2(L_2O)(H_2O)}$, and this undergoes deprotonation to give an inactive catalyst $\mathbf{Zn_2(L_2O)(HO^-)}$. In this case, $\mathbf{Zn_2(L_2O)(H_2O)}$ is specific for cleavage of the O-2-ionized substrate. The relevant proposed pathway involves the deprotonated substrate 2-hydroxypropyl group directly coordinating to the zinc ion followed by a nucleophilic attack on the phosphorus center.[28,29] The only difference between these two cases involves the position of a proton, and the kinetic analysis cannot clearly distinguish these two possible forms for the active catalyst.[44a]

In fact, the uncertainty of the structure and properties of the active form of the complex involves the binding mode of the substrate-catalyst complex. We explored several possible binding modes that were based on the results of previously reported kinetic, spectroscopic, and crystallographic studies of Richard and co-workers.[28,43,44] We then used DFT computations to

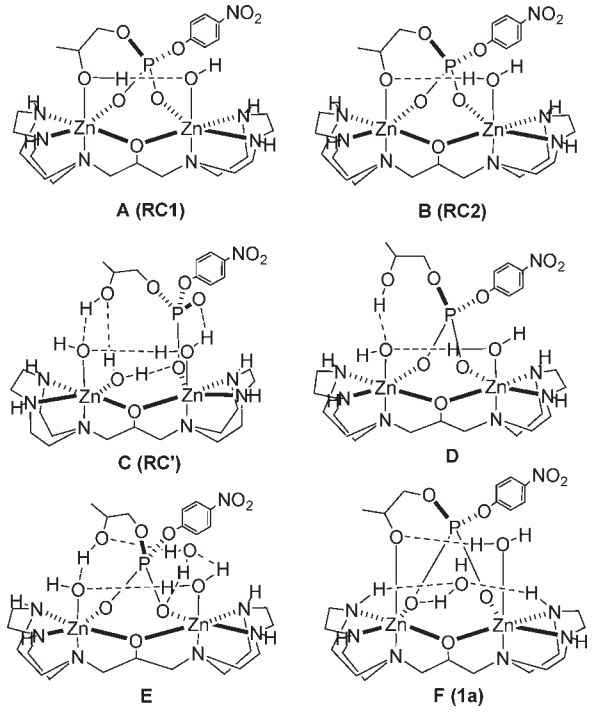

Figure 1. Schematic representations of the possible binding modes of the substrate-catalyst complex are shown (the **F** binding mode was cited from the most favored binding mode '1a' of Fan and Gao's work (ref 45)). The relative free energies for the typical structures are provided at the level of B3LYP/6-311++G(d, p)(SDD for Zn)//B3LYP/6-31G(d, p)(SDD for Zn). (**A**+2$\mathbf{H_2O}$ 0.0 kcal/mol; **B**+2$\mathbf{H_2O}$ 0.0 kcal/mol; **C** 14.8 kcal/mol; **D**+1$\mathbf{H_2O}$ 11.5 kcal/mol; **E** 20.6 kcal/mol; **F**+1$\mathbf{H_2O}$ 15.4 kcal/mol).

explore the possible reaction mechanisms for these binding modes to determine which one gave the most energetically favorable reaction pathway.

Coordination and Binding Modes. Based on the crystal structure of Richard and co-workers,[43a] there are four coordination sites on each Zn(II) center occupied by $\mathbf{L_2O}$ in the catalyst $\mathbf{Zn_2(L_2O)}$, leaving two available coordination sites per metal center for catalysis. In neutral aqueous solution, the remaining coordination sites of $\mathbf{Zn_2(L_2O)}$ may be filled by water molecules. Previous experimental work did not give clear structural and spectroscopic evidence for the specific interactions of the substrate-catalyst complex involved in the mechanism for the cleavage reaction of **HpPNP** catalyzed by $\mathbf{Zn_2(L_2O)}$. In this study, we found a binding mode, that is, the phospate ester binds simultaneously to both zinc centers as a bridge ligand, where each oxygen arm of phosphate coordinates to one zinc center, respectively, and the nucleophilic 2-hydroxypropyl group coordinates to one of the zinc ions while the hydroxide from deprotonation of a water molecule coordinates to the other zinc ion (see Figure 1A, **RC1**). This binding mode is very easily exchanged to form another more interesting binding mode (see Figure 1B, **RC2**) via a proton-transfer process.

In addition, we found another possible binding mode in which one available coordination site is occupied by one of the phosphate oxygen atoms, and the other three available coordination sites are occupied by two water molecules and one hydroxide from deprotonation of a water molecule. For this binding mode the whole complex was connected by hydrogen-bond network (see Figure 1C, **RC′**). **RC′** corresponds to **RC1** with addition of

Scheme 2. Concerted Mechanism (Path I) for the Cleavage of HpPNP Promoted by the Dinuclear Zn(II) Complex of $\mathbf{Zn_2(L_2O)}$[a]

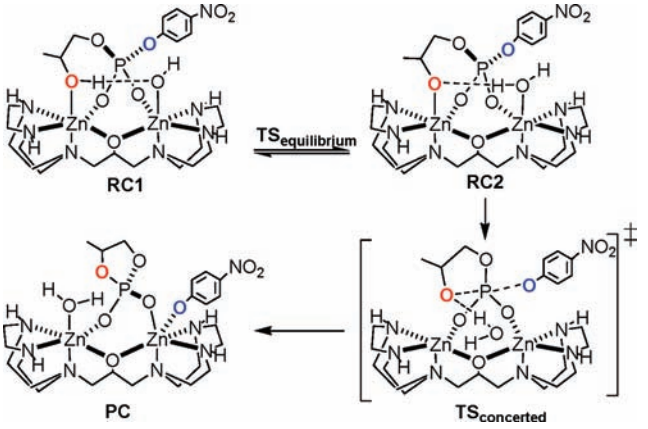

[a] Positions at which kinetic isotope effects were signed. $^{18}k_{Nuc}$ indicates the ^{18}O KIE at the nucleophilic oxygen (red color); $^{18}k_{LG}$ indicates the ^{18}O KIE at the leaving oxygen (blue color).

two water molecules, although there are minor differences in the coordination conditions. The difference between the relative free energies for the **RC1**+2$\mathbf{H_2O}$ system and **RC′** is less than 0.5 kcal/mol at the B3LYP/6-31G(d, p)(SDD for Zn) level of theory. However, when the diffuse functions on heavy atoms are included, the latter system was found to be 14.8 kcal/mol higher than the former system at the B3LYP/6-311++G(d, p)(SDD for Zn)//B3LYP/6-31G(d, p)(SDD for Zn) level of theory. At the same time, we also examined other possible binding modes (see Figure 1D and 1E), and the relative free energies of those were found to be 4.7 and 7.2 kcal/mol higher, respectively, than the **RC1**+2$\mathbf{H_2O}$ system, while the differences between them increased to be 11.5 and 20.6 kcal/mol higher, respectively, than the **RC1**+2$\mathbf{H_2O}$ system when the diffuse functions on heavy atoms were included. It is noteworthy that another possible binding mode has been proposed by Fan and Gao.[45] Figure 1F is the most favored binding mode '1a' determined in the work of Fan and Gao, and this corresponds to **RC2** with addition of one water molecule. However, as Fan and Gao proposed that the fewer-water pathway is more favored when the entropy change and the solvation effects are considered (these phenomena are also present in our calculations and results), the relative free energy of '**1a**' is 15.4 and 9.4 kcal/mol higher than the **RC1**+2$\mathbf{H_2O}$ system (or the **RC2**+2$\mathbf{H_2O}$ system) in the presence/absence of the diffuse functions. This indicates that the binding modes for the **RC′**, the Figure 1D and 1E, and '**1a**' become significantly more disfavored than the **RC1**+2$\mathbf{H_2O}$ system (or the **RC2**+2$\mathbf{H_2O}$ system) when the diffuse functions are included on the heavy atoms in the calculations.

Concerted Mechanism for the Cleavage of HpPNP Promoted by the Dinuclear Zn(II) Complex (Path I). This mechanism and the structures and relative free energy profiles determined for it are depicted in Scheme 2 and in Figure 2 and 3, respectively. In **RC1**, each terminal phosphoryl oxygen atom binds to one zinc center, respectively, and the nucleophilic 2-hydroxypropyl group coordinates to one of the zinc ions while the hydroxide from deprotonation of a water molecule coordinates to the other zinc ion (see **RC1** in Figure 2). $\mathbf{TS_{equilibrium}}$ in Scheme 2 and Figure 2 is the transition state for the hydrogen

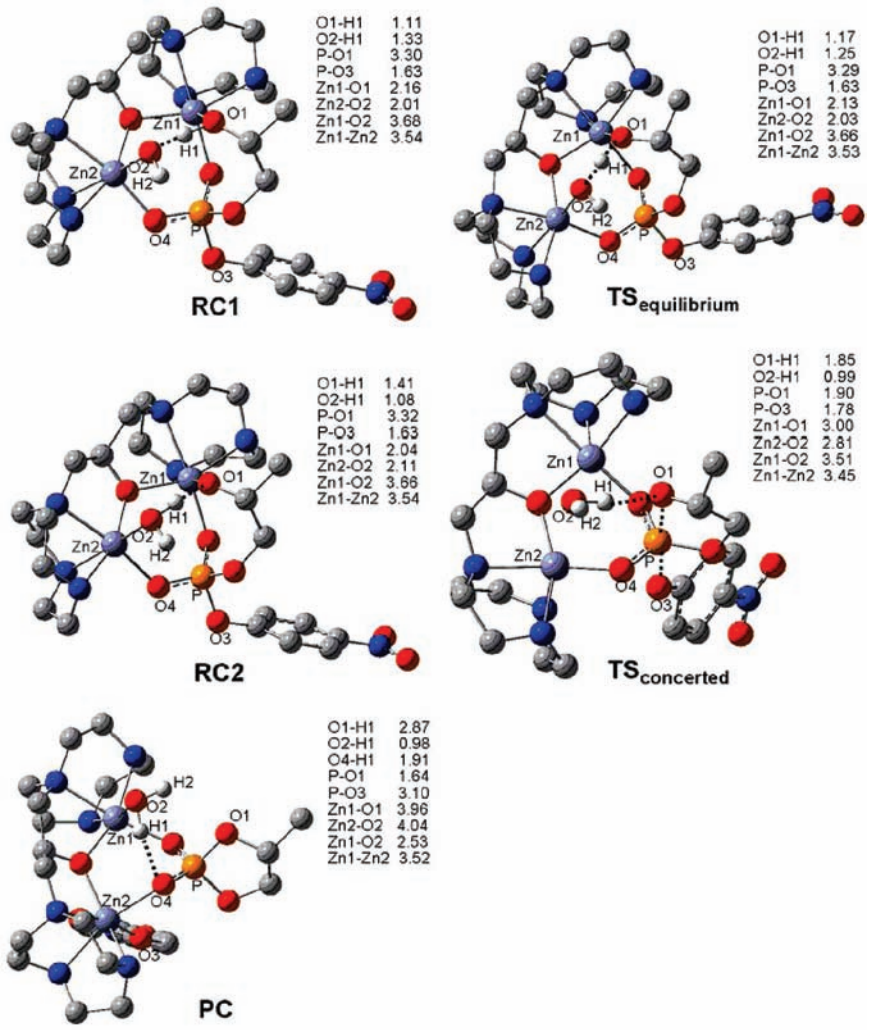

Figure 2. Depicted are optimized structures for the cleavage of **HpPNP** catalyzed by $\mathbf{Zn_2(L_2O)}$ through a concerted mechanism (**Path I**) as shown in Scheme 2. Some hydrogen atoms are omitted for clarity. The distances are in Å.

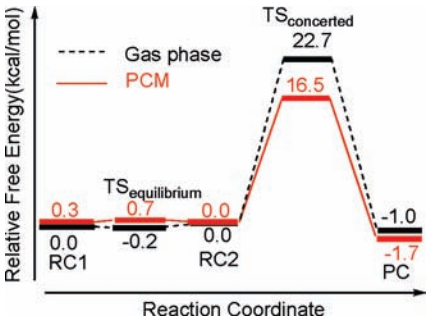

Figure 3. Shown are free energy profiles for the cleavage of **HpPNP** catalyzed by $\mathbf{Zn_2(L_2O)}$ through a concerted mechanism (**Path I**) as shown in Scheme 2.

transfer process between **RC1** and **RC2**. In this transition state, H1 is transferring to the coordinating hydroxide to form a water molecule. The O1−H1 distances in **RC1**, $\mathbf{TS_{equilibrium}}$, and **RC2** are 1.11, 1.17, and 1.41 Å, respectively. The relative free energies along the reaction pathway show that the Zn-coordinated hydroxide deprotonates the nucleophilic 2-hydroxypropyl group via an essentially barrierless transition state ($\mathbf{TS_{equilibrium}}$) and the relative free energies of **RC1** and **RC2** are almost identical. This indicates that the deprotonation of the nucleophilic 2-hydroxypropyl group occurs in a pre-equilibrium step. The flexibility of **RC1** and **RC2** provides evidence that both of the forms of the catalyst, $\mathbf{Zn_2(L_2O)(H_2O)}$ and $\mathbf{Zn_2(L_2O)(HO^-)}$, are also easily exchanged.

Then, with the movement of the coordinating water molecule away from the Zn2, the nucleophilic oxygen O1 of **HpPNP** attacks the phosphorus atom to form a dianionic trigonal bipyramidal phosphorus transition state ($\mathbf{TS_{concerted}}$ in Scheme 2 and Figure 2), in which the coordinating water molecule departs from the Zn2 center. More interestingly, the Zn ion coordination number changed from six in **RC2** to five in this $\mathbf{TS_{concerted}}$, that is, each of the two metal centers is chelated to a triazamacrocycle, alkoxide, and one of the phosphate oxygen atoms with an overall distorted square pyramidal geometry. Subsequently, the leaving group coordinates to Zn2 with cleavage of the P−O2 bond and simultaneously the water molecule coordinates to Zn1 to form **PC**. The P−O1 distances in **RC2**, $\mathbf{TS_{concerted}}$, and **PC** are 3.32, 1.90, and 1.64 Å, respectively. Though the potential of the imaginary normal mode of vibration corresponding to the $\mathbf{TS_{concerted}}$ is soft, the intrinsic reaction coordinate (IRC) calculations along

dx.doi.org/10.1021/ja106456u |*J. Am. Chem. Soc.* 2011, 133, 2904–2915

the reaction coordinate for $\mathbf{TS_{concerted}}$ clearly indicate the direct connection between **RC2** and **PC** (see Figure S1 in the Supporting Information). The highest energy species is the transition state $\mathbf{TS_{concerted}}$ and the overall activation free energy is 22.7 kcal/mol in the gas phase, while the barrier decreases to 16.5 kcal/mol when the effects of solvation are included using the PCM model. NBO analysis shows that both the negative charge of the substrate and the positive charge of the catalyst core are increased in the $\mathbf{TS_{concerted}}$ compared to **RC2** (see Table S3 in the Supporting Information). This indicates that there are some electrostatic interactions between the substrate and the catalyst core that can provide stabilization of the $\mathbf{TS_{concerted}}$. Interestingly, from **RC2** to $\mathbf{TS_{concerted}}$, the negative charge of the nucleophilic oxygen decreases slightly while that of the leaving oxygen shows a corresponding increased. This demonstrates that there is a little shift in the negative charge away from the nucleophilic oxygen and onto the leaving group, which provides qualitative support for Hengge's experimental results.[28] The pH-rate profile[44c] for the cleavage of **HpPNP** catalyzed by $\mathbf{Zn_2(L_2O)}$ shows that the free energy of activation is 18.8 kcal/mol at neutral pH (17.6 kcal/mol at high pH),[59] which is not much higher than the value of 16.5 kcal/mol obtained from our calculations for the concerted mechanism. Most importantly, our calculations demonstrate that **RC2** is the critical active species in the mechanism proposed by Scheme 2. **RC1** is not so critical; it has to convert to the active species **RC2** via a pre-equilibrium prior to the nucleophilic attack step. This result provides further support that the $\mathbf{Zn_2(L_2O)(H_2O)}$ species is the true active form as concluded by Richard and co-workers.[44a]

Calculations of the Isotope Effects. The accuracy of the computational models determines the accuracy of the calculated isotope effects (IEs). Several studies that have established that the frequencies and IEs calculated using B3LYP accurately reflect molecular structure.[60,61] In particular, to test the reliability of the computational method, Hengge and co-workers calculated the EIEs for the deprotonation of *p*-nitrophenol and compared these with their experimental values.[28,62] In this paper, we directly compute the EIEs between the **RC1** and **RC2** of the pre-equilibrium step structures. The ^{18}O EIE and ^{15}N EIE for the deprotonation of **RC1** to form **RC2** are 1.0128 and 1.0000, respectively, which are lower than the calculated values of deprotonation of the **HpPNP** in the absence of the catalyst.[63] This is consistent with the previous experimental result[64] that indicates metal coordination would reduce the EIE for deprotonation. Therefore, this validates that the nucleophic 2-hydroxypropyl group coordinates to one of the zinc ions.

The nucleophile approach and/or the leaving group departure contribute to the KIEs. This permits an analysis of the extent of nucleophile bond formation, leaving group bond cleavage and charge development in the transition state;[28] DFT calculations were also utilized to study the kinetic isotope effect on the concerted mechanism for the cleavage of **HpPNP** promoted by the dinuclear Zn(II) complex of $\mathbf{Zn_2(L_2O)}$. The results from the calculation of the nucleophile ^{18}O KIE and leaving ^{18}O KIE for the concerted mechanism are in good agreement with the experimental values[28] (see Scheme 2 and Table 1 for details).

The calculated value of the nucleophile KIEs in Table 1 is 0.9926 (comparable to the experimental value[28] of 0.9874), which reflects the fractionation of the oxygen isotope for the kinetic effect on the nucleophilic attack. The inverse KIEs show a late transition state and that bond formation is sufficiently far advanced. This evidence is consistent with our optimized

Table 1. Results from the KIE Calculations for the Catalyzed Concerted Mechanism for Cleavage of HpPNP Promoted by the Dinuclear Zn(II) Complex of the $Zn_2(L_2O)$ Catalyst and the Uncatalyzed Mechanism Are Compared with the KIE Experimental Values

	$^{18}k_{Nuc}$	$^{18}k_{LG}$
Cat(calculation)[a]	0.9926	1.0042
Cat(experiment)[b]	0.9874	1.0113
Uncat(calculation)[a]	1.0182	1.0021
Uncat(experiment)[b]	1.0079	1.0064

[a] KIE calculations in this work. [b] KIE experimental values were cited from Hengge's work (ref 28).

structure of $\mathbf{TS_{concerted}}$, in which the forming bond has a length of 1.90 Å while the breaking bond has a length of 1.78 Å. In addition, a previous experimental report also suggested that the nucleophilic oxygen might coordinate to zinc as deduced from an inverse effect.[28] Together with the smaller EIE for deprotonation of the **HpPNP** in the presence of the catalyst, it is thus theoretically reliable that each terminal phosphoryl oxygen atom binds to one zinc center, respectively, and the nucleophilic 2-hydroxypropyl group coordinates to one of the zinc ions while the hydroxide from deprotonation of a water molecule coordinates to the other zinc ion can be applicable to the reaction examined here.

The leaving ^{18}O KIE is used to measure the extent of P−O bond fission. The experimental value[28] of the leaving ^{18}O KIE is 1.0113, which is close to our calculated value of 1.0042. Its magnitude is close to unity for a transition state that has a bond fission character for the leaving group. Fission of the P−O bond results in a negative charge on the leaving group in the transition state. NBO analysis is consistent with the leaving ^{18}O KIE, which further supports a concerted mechanism.

Analysis of the Role of the Catalyst. To further understand the role of the catalyst, we compare the **HpPNP** cleavage reaction mechanisms in the presence/absence of the catalyst. A detailed analysis of the geometric and the electronic structure along the both reaction pathways provides some detailed insights into how the catalyst affects the substrate throughout the reaction and potentially alters the reaction mechanism. Previous experimental studies[28] demonstrated that the **HpPNP** cleavage mechanism in the absence of catalyst is a specific-base mechanism, in which the deprotonation of the nucleophilic 2-hydroxypropyl group takes place in a pre-equilibrium step followed by a nucleophilic attack on the phosphorus center. Therefore, it is feasible to make an individual discussion for the separate steps of deprotonation and nucleophilic attack. Unfortunately, in a dissociation reaction, the accurate theoretical prediction of the pK_a values or the free energy change for the deprotonation in solution is still a difficult and challenging task.[65,66] Instead, we used an experimental pK_a value[67] to estimate the calculated free energy change (about 17.7 kcal/mol) for the deprotonation of the nucleophilic 2-hydroxypropyl group of **HpPNP**.[68] Comparison of this value (although it is a rough estimate) to the free energy change value (lower than 1.0 kcal/mol) between **RC1** and **RC2** shows that deprotonation of **HpPNP** is obviously much more favored with the help of the catalyst. That is, acting as a Lewis acid, the catalyst facilitates the deprotonation of **HpPNP** as well as significantly increases the nucleophilic reactivity for subsequent attack. This result provides further support for the experimental observation[44a] about the solvent deuterium isotope effect. After the deprotonation of

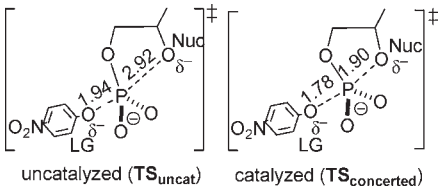

Figure 4. Schematic representations of the altered transition state structures for the cleavage of **HpPNP** through a concerted mechanism in the absence or presence of the catalyst $\mathbf{Zn_2(L_2O)}$. The numbers refer to bond length (Å).

HpPNP, the uncatalyzed reaction will proceed through a nucleophilic attack with a concerted transition-state ($\mathbf{TS_{uncat}}$ in Figure 4 and Figure S2 in the Supporting Information). If we set the free energy of **HpPNP** as a reference point, the total activation barrier for the uncatalyzed reaction is calculated to be about 23.2 kcal/mol, which is comparable to the experimentally observed values (28.3 kcal/mol at neutral pH).[44c,59]

Comparisons of the geometry parameters of the transition state between the catalyzed and uncatalyzed reactions will help to reveal the role of the catalyst. The cleavage of **HpPNP** catalyzed by $\mathbf{Zn_2(L_2O)}$ proceeds through a transition state structure that is significantly different from that of the uncatalyzed reaction (Figure 4). The total in-line distance between the O_{Nuc} atom and the O_{LG} atom is lowered by 24.3% (from 4.86 Å in $\mathbf{TS_{uncat}}$ to 3.68 Å in $\mathbf{TS_{concerted}}$). More importantly, the distance of the P−O_{Nuc} (1.90 Å) in $\mathbf{TS_{concerted}}$ is significantly shortened by 34.9% in comparison with that of the uncatalyzed reaction (2.92 Å), whereas the distance of P−O_{LG} (1.78 Å) in $\mathbf{TS_{concerted}}$ is only 8.2% shorter than that of the uncatalyzed reaction (1.94 Å). The change of the key geometric parameters for the transition state indicates that the $\mathbf{TS_{concerted}}$ is a far more associative or tight transition state, compared to the $\mathbf{TS_{uncat}}$ in the uncatalyzed reaction.

NBO analysis also reveals useful information. Comparison of the changes of the bond lengths shows a similar but more direct correlation from the NBO P−O normalized bond orders (see Figure S3 in the Supporting Information). The P−O_{Nuc} bond order significantly increases from 0.12 in $\mathbf{TS_{uncat}}$ to 0.65 in $\mathbf{TS_{concerted}}$, while the P−O_{LG} bond order changes only slightly from 0.55 to 0.76. More importantly, the sum of the bond orders to the nucleophile and leaving group in $\mathbf{TS_{uncat}}$ is 0.67 (less than 1), while this sum in $\mathbf{TS_{concerted}}$ is up to 1.41 (greater than 1). It is clear that the catalyst significantly alters the loose transition-state ($\mathbf{TS_{uncat}}$) to an associative or tight transition-state ($\mathbf{TS_{concerted}}$).[69] Furthermore, the NBO analysis of $\mathbf{TS_{concerted}}$ shows a stronger interaction[70] (41.0 kcal/mol versus 11.9 kcal/mol of $\mathbf{TS_{uncat}}$) between the lone pair orbital of the nucleophilic O_{Nuc} atom and the antibond orbital of the P−O_{LG} (or the empty developing orbital on P), which is not present either in **RC2** or in $\mathbf{HpPNP^-}$. This stronger interaction further reflects that more nucleophilic bond formation in the $\mathbf{TS_{concerted}}$ with the help of catalyst. Besides, the NBO charges of the two terminal phosphoryl oxygens become more negative, while the charge difference of the O_{Nuc} atom is almost negligible in the $\mathbf{TS_{concerted}}$ (compared to that of $\mathbf{TS_{uncat}}$), suggesting that the catalyst provides a prior charge stabilization at the two terminal phosphoryl oxygens, compared with the O_{Nuc} atom. On the other hand, both the negative charge of the O_{LG} atom and the positive charge of the P atom in the $\mathbf{TS_{concerted}}$ (compared to that of $\mathbf{TS_{uncat}}$) are increased. This result indicates that there is negative charge accumulation at the O_{LG} atom. In summary, the catalyst induces the more negative charge accumulation at the leaving group, compared to the nucleophilic group.

Scheme 3. Stepwise Mechanism (Path II) for the Cleavage of HpPNP Promoted by the Dinuclear Zn(II) Complex of $\mathbf{Zn_2(L_2O)}$[a]

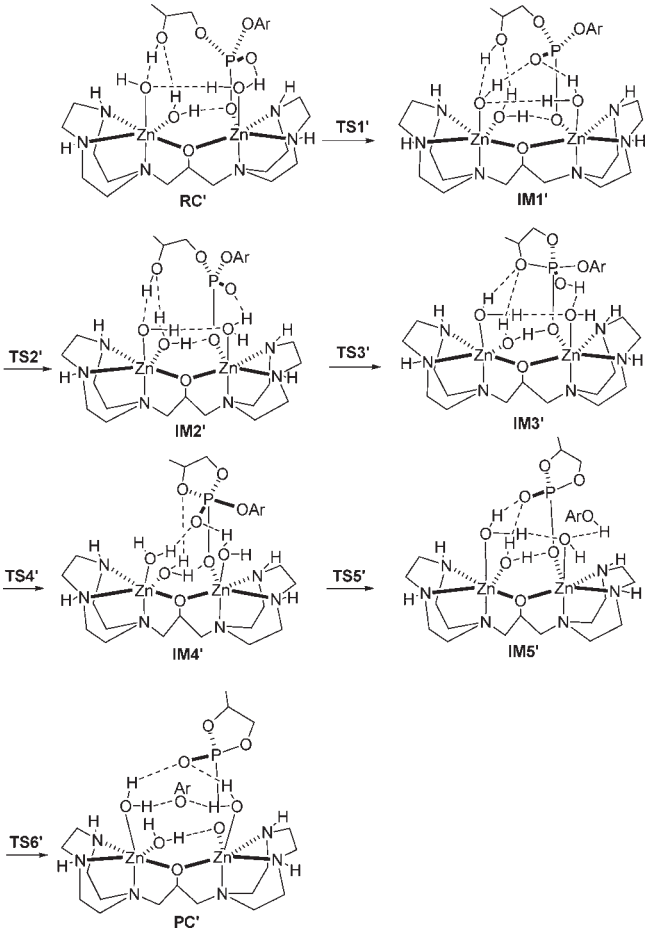

[a] Ar = *p*-nitrophenyl group.

The KIE's analysis also provides more profound information (Table 1). With or without the catalyst, the reasonable agreement of the calculated and the experimental values of the nucleophile ^{18}O KIE and leaving ^{18}O KIE reflects the reliability of our calculations (Table 1). Generally, a greater nucleophilic ^{18}O KIE is accompanied by an earlier transition-state with a looser nucleophilic bond formation. Surprisingly, from the uncatalyzed to the catalyzed reaction mechanism, the change of the nucleophilic ^{18}O KIE from normal (1.0182) to inverse (0.9926) indicates the catalyst causes the P−O_{Nuc} binding in the transition-state to alter from loose to highly tight, that is, there is a transformation from an early transition-state to a late transition-state in the presence of the catalyst. On the other hand, the relatively increased leaving group KIEs (1.0042 for the catalyzed reaction compared to 1.0021 for the uncatalyzed reaction) indicates that the negative charge accumulation at the O_{LG} atom and a relatively larger P−O_{LG} fission in the catalyzed reaction. Above all, both of the catalyzed and uncatalyzed reactions go through concerted mechanisms; however, the catalyst alters the transition state to become significantly more associative or tight, that is, bond formation to the nucleophile is remarkably more advanced than leaving group bond fission in the catalyzed mechanism.

dx.doi.org/10.1021/ja106456u |*J. Am. Chem. Soc.* 2011, 133, 2904–2915

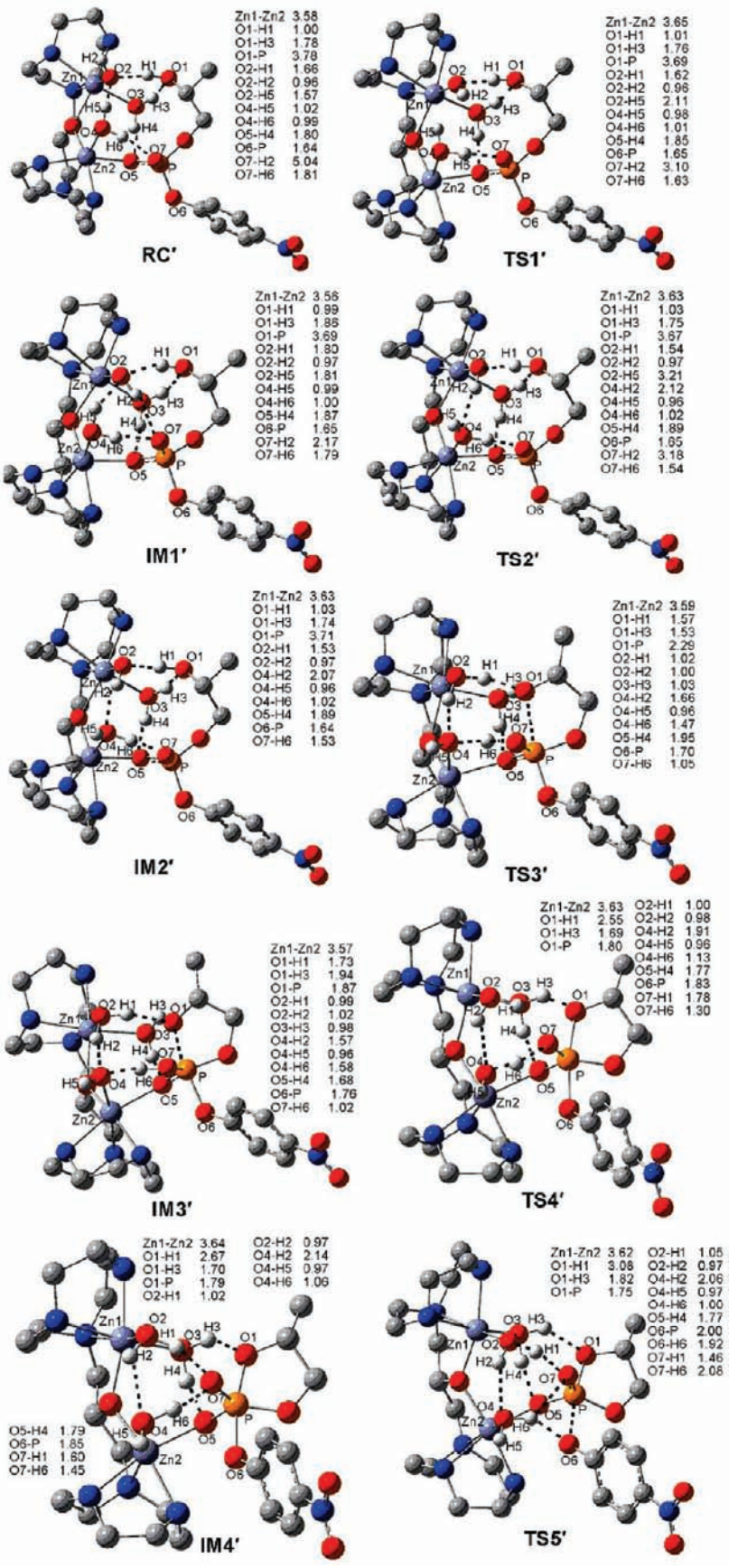

Figure 5. Continued

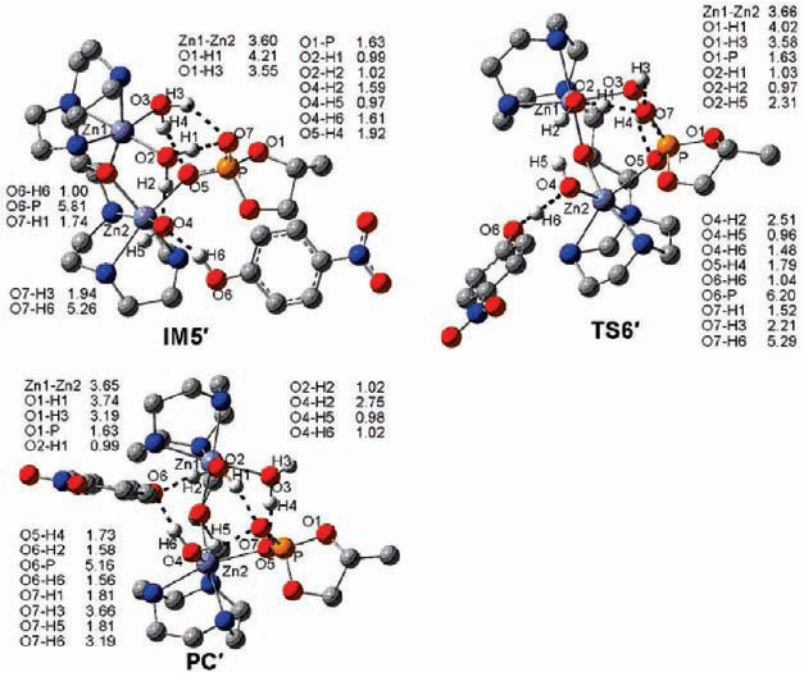

Figure 5. Depictions are shown of the optimized structures for the cleavage of **HpPNP** catalyzed by $\mathbf{Zn_2(L_2O)}$ through the stepwise mechanism (**Path II**) as shown in Scheme 3. Some hydrogen atoms are omitted for clarity. The distances are in Å.

Stepwise Mechanism for the Cleavage of HpPNP Promoted by the Dinuclear Zn(II) Complex (Path II). An alternative pathway and the structures determined for it are depicted in Scheme 3 and in Figure 5, respectively. In this mechanism the substrate binds to one of the Zn centers to form a six-coordinated complex (**RC′**) with an octahedral geometry that includes hydrogen bonds O1−H1···O2, O3−H3···O1, O3−H4···O5, O4−H5···O2, and O4−H6···O7. **TS1′** in Scheme 3 and Figure 5 is the transition state for the change of position of the hydrogen H2 in the coordinating water network to produce **IM1′** in which a new hydrogen bond O2−H2···O7 formed. **TS2′** in Scheme 3 and Figure 5 is the transition state for the change of position of the hydrogen atoms H2 and H5 in the coordinating water network to form **IM2′** in which the hydrogen bond between O2 and H5 is broken to form another one between O4 and H2 and at the same time the hydrogen bond O2−H2···O7 is also broken. **TS3′** in Scheme 3 and Figure 5 is the transition state for the attack of O1 against the phosphorus atom to form the five-coordinated phosphorus intermediate **IM3′**. In this transition state, the fifth P−O bond is in the process of being formed (the P−O1 distance is 2.29 Å), H1 is exchanging between O1 and O2, and H6 has already transferred to O7. **TS4′** in Scheme 3 and Figure 5 is the transition state between **IM3′** and **IM4′**, in which H6 interacts with both O4 and O7, for the rotation of the coordinating water molecule by Zn1−O2 bond to form **IM4′**. Subsequently, the hydrogen bond between O1 and H1 is broken and reformed between O7 and H1 as shown in **IM4′**, in which the hydrogen H6 transfers back to O4. In **TS5′**, with the rotation of the coordinating water molecule by the Zn2−O4 bond, the entire PO_5unit rotates around the P−O5 bond while H6 is moving its hydrogen bond from O7 to O6. At the same time, the P−O6 bond is breaking and the cyclic phosphodiester and the *p*-nitrophenylate are in the process of forming. Then, after the hydrogen atom H6 moves to O6, the **IM5′** forms. Finally, via **TS6′**, with the movement of the hydrogen atoms H5 and H2 and the transfer of hydrogen H6, the entire PO_5unit rotates back around the P−O5 bond and the *p*-nitrophenylate ion forms although the PO_5unit and the *p*-nitrophenylate ion are still bound to the Zn centers and the ligands in **PC′**.

The relative free energies along the reaction pathway shown in Scheme 3 are listed in Figure 6. In the gas phase, the highest energy species is the transition-state **TS5′** with an overall activation free energy of 32.0 kcal/mol. This barrier decreases to 21.3 kcal/mol when the effects of solvation are included using the PCM water model. In aqueous solution, the barrier for the attack of O2 against the phosphorus atom accompanied with the deprotonation of the nucleophilic 2-hydroxypropyl group (**TS3′**) is 22.3 kcal/mol, which is almost the same in the gas phase (22.4 kcal/mol). This result demonstrates that the **Path II** depicted in Scheme 3 is a general base catalysis mechanism.

In the whole catalysis cycle (from **RC′** to **PC′**), the NBO charge of the catalyst $\mathbf{Zn_2(L_2O)}$ is almost unchanged, and the negative charge moves mainly from the $\mathbf{H_2O}$ moiety into $\mathbf{HpPNP^-}$ (see Table S5 in the Supporting Information). The negative charge of $\mathbf{HpPNP^-}$ in the determining-step transition state of the stepwise mechanism is significantly lower than that for the concerted mechanism. This may suggest that the electrostatic interaction between the substrate and the catalyst core of the stepwise mechanism is weaker than that of the concerted mechanism.

Concerted or Stepwise Mechanism? Systematic Comparisons of Proposed Pathways. Previous experimental reports speculated that the cleavage mechanism of **HpPNP** promoted by $\mathbf{Zn_2(L_2O)}$ might take place via a concerted mechanism[28] and has a specific-base catalysis character.[44a] However, very recently, another possible pathway (**Path FG**) has been proposed by Fan and Gao[45] using a theoretical study[71] via a general base catalytic mechanism and a stepwise mechanism, which is significantly different from the experimental observation.[28,44a] For the sake of a more thorough comparison and discussion, we

dx.doi.org/10.1021/ja106456u |*J. Am. Chem. Soc.* 2011, 133, 2904–2915

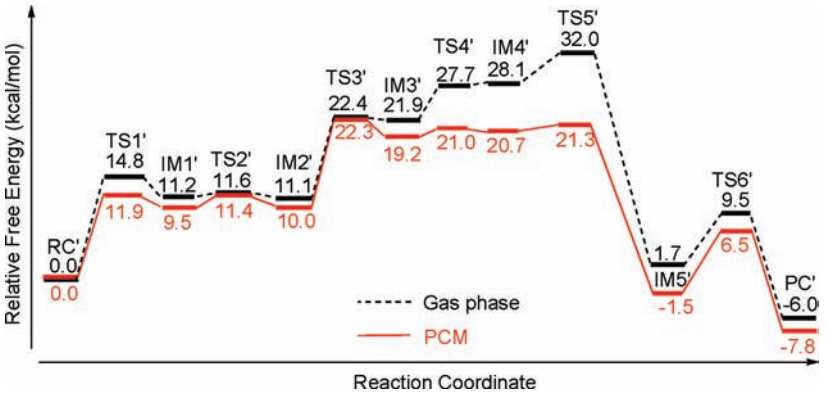

Figure 6. Shown are free energy profiles for the cleavage of **HpPNP** catalyzed by $\mathbf{Zn_2(L_2O)}$ through the stepwise mechanism (**Path II**) as shown in Scheme 3.

Table 2. Comparison of the Relative Free Energies (kcal/mol) for the Starting Complexes and the Key Transition States for the Concerted and Stepwise Pathways

	concerted mechanism (Path I, one-water pathway)[a]		stepwise mechanism (Path II, three-water pathway)[a]			stepwise mechanism (Path FG, two-water pathway)[b]		
	RC2+2H$_2$O	TS$_{concerted}$+2H$_2$O	RC′	TS3′	TS5′	1a+1H$_2$O	TS2+1H$_2$O	TS3+1H$_2$O
B3LYP/6-31G(d,p)[c]	0	16.5	-0.2	22.2	21.1	9.4	19.8	18.1
B3LYP/6-31+G(d,p)[c]	0	14.4	12.5	36.6	29.0	14.6	24.5	19.9
B3LYP/6-311++G(d,p)// B3LYP/6-31G(d,p)[c]	0	16.2	14.8	39.4	36.8	15.4	27.1	21.4
BHandHLYP/6-31G(d,p)[c]	0	18.8	2.0	27.5	24.7	10.6	22.8	23.2
BHandHLYP/6-311++G(d,p)// BHandHLYP/6-31G(d,p)[c]	0	18.8	14.2	41.5	37.8	15.2	29.0	29.9
TPSS/6-31G(d,p)[c]	0	12.5	-2.5	11.8	13.8	8.1	15.4	NA[d]
TPSS/6-311++G(d,p)// TPSS/6-31G(d,p)[c]	0	12.2	12.0	28.2	29.1	13.9	22.6	NA[d]

[a] This work. [b] All the species in this pathway proposed by Fan and Gao (ref 45) was recalculated at the current level of theory. [c] SDD for Zn. [d] Not located in this level of theory.

recalculated the starting complex structure of '**1a**' and all the transition states of **Path FG** using the B3LYP, the BHandHLYP, and the TPSS functionals with the 6-31G(d, p)(SDD for Zn) basis set for the geometry and frequency calculations followed by single point energy refinement with the 6-311++G(d, p)(SDD for Zn) basis set, respectively. The starting complex '**1a**' corresponds to **RC2** with the addition one water molecule. If we set the (**RC2**+$\mathbf{H_2O}$) system as a reference point, the relative free energy of '**1a**' is calculated to be 15.4, 16.2, and 14.6 kcal/mol and the relative free energies of the highest energy species in **Path FG** are calculated to be 25.8, 29.0, and 23.3 kcal/mol, while the barrier in **Path I** is 16.2, 18.8, and 12.2 kcal/mol using the B3LYP, the BHandHLYP, and the TPSS functionals with the 6-311++G(d, p)(SDD for Zn)//6-31G(d, p)(SDD for Zn) basis set, respectively (see Table 2). The calculated reaction barriers are generally similar to each other (the energy barrier in the **Path FG** is 10.4−11.1 kcal/mol higher than that of **Path I** at the same larger basis set) with the three different methods, while the reaction barriers of B3LYP and BHandHLYP functionals gave the better agreement with experimental results[44c] where the free energy of activation is 18.8 kcal/mol at neutral pH (17.6 kcal/mol at high pH).[59] It appears that the calculations using the TPSS functional more severely underestimates the reaction barrier for this type of reaction system. For the individual pathway such as **Path I**, **Path II**, or **Path FG**, additional diffuse functions on the heavy atoms appears to not obviously influence the reaction barrier. We also reoptimized the key structures at the B3LYP/6-31+G(d, p)(SDD for Zn) level of theory, and these results are similar to those obtained from the B3LYP/6-311++G(d, p)(SDD for Zn) single-point calculations based on the optimized geometries from the B3LYP/6-31G(d, p)-(SDD for Zn) calculations. However, if we compared all of the pathways at the same reference point, using the diffuse functions on the heavy atoms seems to have a large effect for the **Path II** and the **Path FG** when the entropy change and the solvation effects are considered. The relative free energies for the starting complex and the determining-step transition state in **Path II** and **Path FG** become much higher, while those of **Path I** are almost unchanged with larger basis sets. This provides further support that the reaction barrier of **Path I** is significantly lower than those of **Path II** and **Path FG**.

Notably, there are one-, two-, and three-water molecule(s) in the **Path I**, **Path FG**, and **Path II** reaction mechanisms, respectively. As Fan and Gao proposed that the fewer-water pathway is more favored when the entropy change and the solvation effects are considered (these phenomena are also present in our calculations and results). It is clear that **Path I** is more favored than **Path FG**, while **Path II** has the highest free energy of activation (Table 2). A conclusion by Fan and Gao opposite with the experimental observation appears to happen because of the difficulty in not being able to locate a suitable fewer-water pathway in the theoretical study. In addition, compared to **Path**

dx.doi.org/10.1021/ja106456u |*J. Am. Chem. Soc.* 2011, 133, 2904–2915

I and **Path FG** mechanisms, replacing one arm of the phosphoryl group and the nucleophilic 2-hydroxypropyl group of the substrate, the water molecules coordinate to the Zn centers in the **Path II** mechanism which decreases the interaction of the substrate-catalyst system and increases the relative free energy of the determining-step transition states.

In brief, the energy barrier for the concerted mechanism presented here is significantly lower than that of the alternative multistep mechanisms with two or three water molecules. Most importantly, including the structures, free energy profiles, charges and the KIEs, the good agreement of the calculated and experimental data suggests that the concerted mechanism (**Path I**) is the most favored and reliable reaction pathway of those considered.

CONCLUSIONS

We have reported a DFT computational study of the reaction mechanism for the cleavage of a RNA model, **HpPNP**, catalyzed by $\mathbf{Zn_2(L_2O)}$. Previous studies have not focused on characterizing the structure and properties of the binding mode of the substrate-catalyst complex and the nucleophile coordination. Our investigation provides new insight into the interaction of the substrate-catalyst complex, that is, each terminal phosphoryl oxygen atom binds to one zinc center, respectively, and the nucleophilic 2-hydroxypropyl group coordinates to one of the zinc ions and the hydroxide from deprotonation of a water molecule coordinates to the other zinc ion. More importantly, our results indicate a concerted mechanism. To our knowledge, this is the first theoretical evidence for the concerted mechanism of a phosphate cleavage mediated by a dinuclear zinc metal complex, although there have been a few previous experimental reports which speculated that the cleavage mechanism of **HpPNP** promoted by $\mathbf{Zn_2(L_2O)}$ might take place via a concerted mechanism.[28] Calculations of the nucleophile ^{18}O KIE and leaving ^{18}O KIE for the concerted mechanism are in good agreement with the experimental values. The energy barrier for the concerted mechanism presented here is 16.5 kcal/mol, and this value is significantly lower than the values found for the alternative multistep mechanisms. Our calculations also indicate this reaction proceeds via a specific-base catalysis mechanism in which the deprotonation of the nucleophilic 2-hydroxypropyl group occurs in a pre-equilibrium step before a nucleophilic attack on the phosphorus center takes place. Together with the structures, free energy profiles, charges and the KIEs, the agreement of the calculated and experimental data suggests that the **Path I** mechanism is the favored reaction pathway. A detailed comparison of the geometric and the electronic structure for the **HpPNP** cleavage reaction mechanisms in the presence/absence of the catalyst revealed that the catalyst significantly altered the determining-step transition state to become far more associative or tight, that is, bond formation to the nucleophile was remarkably more advanced than leaving group bond fission in the catalyzed mechanism. The results reported here has implications for the mechanistic interpretation of dinuclear metal-complex assisted phosphate cleavage in biological systems and in particular for RNA cleavage, which will be helpful for the future design of new metal complexes for the catalyzed phosphate cleavage reaction.

ASSOCIATED CONTENT

Supporting Information. The complete ref 46; the IRC along the reaction coordinate for the $\mathbf{TS_{concerted}}$ (Figure S1); optimized structures for the uncatalyzed reaction mechanism (Figure S2); schematic representation of the altered transition state structures (Figure S3); electronic energies, zero-point energies, enthalpies, free energies (in Hartrees), and solvation free energies (in kcal/mol) for all of the relevant species and the NBO charges (Table S1−S10); Cartesian coordinates (in Å). This material is available free of charge via the Internet at http://pubs.acs.org.

AUTHOR INFORMATION

Corresponding Author
ceszhcy@mail.sysu.edu.cn; phillips@hkucc.hku.hk

ACKNOWLEDGMENT

We gratefully acknowledge the National Natural Science Foundation of China (20673149, 20973204, 20950110326) and Guangdong Provincial Natural Science Foundation (9351027501-000003) to C.Y.Z. and N.J.D., and the Research Grants Council of Hong Kong (HKU 7039/07P) to D.L.P. for financial support of this research. This work was partially sponsored by the high-performance grid computing platform of Sun Yat-sen University. The high performance computing facility at the University of Memphis is also acknowledged. We thank the reviewers for many insightful comments and suggestions.

REFERENCES

(1) Cleland, W. W.; Hengge, A. C. *Chem. Rev.* **2006**, *106*, 3252–3278.

(2) (a) Lopez, X.; Dejaegere, A.; Leclerc, F.; York, D. M.; Karplus, M. *J. Phys. Chem. B* **2006**, *110*, 11525–11539. (b) Lopez, X.; York, D. M.; Dejaegere, A.; Karplus, M. *Int. J. Quantum Chem.* **2002**, *86*, 10–26.

(3) Stivers, J. T.; Nagarajan, R. *Chem. Rev.* **2006**, *106*, 3443–3467.

(4) (a) López-Canut, V.; Roca, M.; Bertrán, J.; Moliner, V.; Tuñón, I. *J. Am. Chem. Soc.* **2010**, *132*, 6955–6963. (b) Elsässer, B.; Valiev, M.; Weare, J. H. *J. Am. Chem. Soc.* **2009**, *131*, 3869–3871. (c) Sharma, S.; Rauk, A.; Juffer, A. H. *J. Am. Chem. Soc.* **2008**, *130*, 9708–9716. (d) De Vivo, M.; Dal Peraro, M.; Klein, M. L. *J. Am. Chem. Soc.* **2008**, *130*, 10955–10962.

(5) Westheimer, F. H. *Science* **1987**, *235*, 1173–1178.

(6) (a) Corona-Martínez, D. O.; Taran, O.; Yatsimirsky, A. K. *Org. Biomol. Chem.* **2010**, *8*, 873–880. (b) Ashkenazi, N.; Zade, S. S.; Segall, Y.; Karton, Y.; Bendikov, M. *Chem. Commun.* **2005**, 5879–5881.

(7) (a) Chen, X.; Zhan, C. -G. *J. Phys. Chem. A* **2004**, *108*, 6407–6413. (b) Florin, J.; Warshel, A. *J. Am. Chem. Soc.* **1997**, *119*, 5473–5474. (c) Dejaegere, A.; Karplus, M. *J. Am. Chem. Soc.* **1993**, *115*, 5316–5317. (d) Tole, P.; Lim, C. *J. Am. Chem. Soc.* **1994**, *116*, 3922–3931.

(8) Krämer, R. *Coord. Chem. Rev.* **1999**, *182*, 243–261.

(9) Molenveld, P.; Engbersen, J. F. J.; Reinhoudt, D. N. *Chem. Soc. Rev.* **2000**, *29*, 75–86.

(10) (a) Mancin, F.; Scrimin, P.; Tecilla, P.; Tonellato, U. *Chem. Commun.* **2005**, 2540–2548. (b) Livieri, M.; Mancin, F.; Tonellato, U.; Chin, J. *Chem. Commun.* **2004**, 2862–2863. (c) Mancin, F.; Tecilla, P. *New J. Chem.* **2007**, 800–817. (d) Bonomi, R.; Selvestrel, F.; Lombardo, V.; Sissi, C.; Polizzi, S.; Mancin, F.; Tonellato, U.; Scrimin, P. *J. Am. Chem. Soc.* **2008**, *130*, 15744–15745.

(11) Chin, J. *Acc. Chem. Res.* **1991**, *24*, 145–152.

(12) (a) Bunn, S. E.; Liu, C. T.; Lu, Z.-L.; Neverov, A. A.; Brown, R. S. *J. Am. Chem. Soc.* **2007**, *129*, 16238–16248. (b) Mohamed, M. F.; Neverov, A. A.; Brown, R. S. *Inorg. Chem.* **2009**, *48*, 11425–11433.

(13) Morrow, J. R.; Iranzo, O. *Curr. Opin. Chem. Biol.* **2004**, *8*, 192–200.

(14) (a) Linjalahti, H.; Feng, G.; Mareque-Rivas, J. C.; Mikkola, S.; Williams, N. H. *J. Am. Chem. Soc.* **2008**, *130*, 4232–4233. (b) Feng, G.; Mareque-Rivas, J. C.; Williams, N. H. *Chem. Commun.* **2006**, 1845–1847.

(15) Ott, R.; Krämer, R. *Appl. Microbiol. Biotechnol.* **1999**, *52*, 761–767.

(16) (a) Lu, Z. -L.; Liu, C. T.; Neverov, A. A.; Brown, R. S. *J. Am. Chem. Soc.* **2007**, *129*, 11642–11652. (b) Neverov, A. A.; Lu, Z. -L.; Marwell, C. I.; Mohamed, M. F.; White, C. J.; Tsang, J. S. W.; Brown, R. S. *J. Am. Chem. Soc.* **2006**, *128*, 16398–16405. (c) Edwards, D. R.; Tsang, W. Y.; Neverov, A. A.; Brown, R. S. *Org. Biomol. Chem.* **2010**, *8*, 822–827.

(17) (a) Yashiro, M.; Ishikubo, A; Komiyama, M. *Chem. Commun.* **1997**, 83–84. (b) Yashiro, M.; Ishikubo, A; Komiyama, M. *J. Chem. Soc., Chem. Commun.* **1995**, 1793–1794. (c) Komiyama, M.; Takeda, N.; Shigekawa, H. *Chem. Commun.* **1999**, 1443–1451.

(18) Hegg, E. L.; Burstyn, J. N. *Coord. Chem. Rev.* **1998**, *173*, 133–165.

(19) Chin, J. *Curr. Opin. Chem. Biol.* **1997**, *1*, 514–521.

(20) Brown, R. S.; Lu, Z.-L; Liu, C. T.; Tsang, W. Y.; Edwards, D. R.; Neverov, A. A. *J. Phys. Org. Chem.* **2010**, *23*, 1–15.

(21) (a) Nwe, K.; Andolina, C. M.; Morrow, J. R. *J. Am. Chem. Soc.* **2008**, *130*, 14861–14871. (b) Nwe, K.; Richard, J. P.; Morrow, J. R. *Dalton Trans.* **2007**, 5171–5178. (c) Farquhar, E.; Richard, J. P.; Morrow, J. R. *Inorg. Chem.* **2007**, *46*, 7169–7177. (d) Mathews, R. A.; Rossiter, C. S.; Morrow, J. R.; Richard, J. P. *Dalton Trans.* **2007**, 3804–3811.

(22) Gunnlaugsson, T.; Nieuwenhuyzen, M.; Nolan, C. *Polyhedron* **2003**, 3231–3242.

(23) (a) Koike, T.; Inoue, M.; Kimura, E.; Shiro, M. *J. Am. Chem. Soc.* **1996**, *118*, 3091–3099. (b) Koike, T.; Kajitani, S.; Nakamura, I.; Kimura, E.; Shiro, M. *J. Am. Chem. Soc.* **1995**, *117*, 1210–1219. (c) Koike, T.; Kimura, E. *J. Am. Chem. Soc.* **1991**, *113*, 8935–8941. (d) Kinoshita, E.; Takahashi, M.; Takeda, H.; Shiro, M.; Koike, T. *Dalton Trans.* **2004**, 1189–1193.

(24) (a) Liu, C. T.; Neverov, A. A.; Brown, R. S. *J. Am. Chem. Soc.* **2008**, *130*, 13870–13872. (b) Liu, C. T.; Neverov, A. A.; Brown, R. S. *Inorg. Chem.* **2007**, *46*, 1778–1788. (c) Liu, C. T.; Neverov, A. A.; Brown, R. S. *J. Am. Chem. Soc.* **2008**, *130*, 16711–16720. (d) Liu, C. T.; Neverov, A. A.; Marwell, C. I.; Brown, R. S. *J. Am. Chem. Soc.* **2010**, *132*, 3561–3573.

(25) Kövári, E.; Krämer, R. *J. Am. Chem. Soc.* **1996**, *118*, 12704–12709.

(26) Schroeder, G. K.; Lad, C.; Wyman, P.; Williams, N. H.; Wolfenden, R. *Proc. Natl. Acad. Sci. U. S. A.* **2006**, *103*, 4052–4055.

(27) Feng, G.; Natale, D.; Prabaharan, R.; Mareque-Rivas, J. C.; Williams, N. H. *Angew. Chem., Int. Ed.* **2006**, *45*, 7056–7059.

(28) Humphry, T.; Iyer, S.; Iranzo, O.; Morrow, J. R.; Richard, J. P.; Paneth, P.; Hengge, A. C. *J. Am. Chem. Soc.* **2008**, *130*, 17858–17866.

(29) Morrow, J. R.; Amyes, T. L.; Richard, J. P. *Acc. Chem. Res.* **2008**, *41*, 539–548.

(30) Livieri, M.; Mancin, F.; Saielli, G.; Chin, J.; Tonellato, U. *Chem.—Eur. J.* **2007**, *13*, 2246–2256.

(31) Oivanen, M.; Kuusela, S.; Lönnberg, H. *Chem. Rev.* **1998**, *98*, 961–990.

(32) Perreault, D. M.; Anslyn, E. V. *Angew. Chem., Int. Ed. Engl.* **1997**, *36*, 432–450.

(33) Feng, G.; Mareque-Rivas, J. C.; de Rossales, R. T. M.; Williams, N. H. *J. Am. Chem. Soc.* **2005**, *127*, 13470–13471.

(34) Fan, Y.; Gao, Y. Q. *J. Am. Chem. Soc.* **2007**, *129*, 905–913.

(35) Wilcox, D. E. *Chem. Rev.* **1996**, *96*, 2435–2458.

(36) Cowan, J. A. *Curr. Opin. Chem. Biol.* **2001**, *5*, 634–642.

(37) (a) Steitz, T. A.; Steitz, J. A. *Proc. Natl. Acad. Sci. U. S. A.* **1993**, *90*, 6498–6502. (b) Pontius, B. W.; Lott, W. B.; Von Hippel, P. H. *Proc. Natl. Acad. Sci. U. S. A.* **1997**, *94*, 2290–2294.

(38) De Iuliis, G. N.; Lawrance, G. A.; Fieuw-Makaroff, S. *Inorg. Chem. Commun.* **2000**, *3*, 307–309.

(39) Sissi, C.; Rossi, P.; Felluga, F.; Formaggio, F.; Palumbo, M.; Tecilla, P.; Toniolo, C.; Scrimin, P. *J. Am. Chem. Soc.* **2001**, *123*, 3169–3170.

(40) Lipscomb, W. N.; Sträter, N. *Chem. Rev.* **1996**, *96*, 2375–2433.

(41) (a) Charette, A. B.; Gagnon, A.; Fournier, J.-F. *J. Am. Chem. Soc.* **2002**, *124*, 386–387. (b) Zhao, C.; Wang, D.; Phillips, D. L. *J. Am. Chem. Soc.* **2002**, *124*, 12903–12914.

(42) The synthesis of this metal-complex's ligand was first reported: Sessler, J. L.; Sibert, J. W.; Burrell, A. K.; Lynch, V.; Markert, J. T.; Wooten, C. L. *Inorg. Chem.* **1993**, *32*, 4277–4283.

(43) (a) Iranzo, O.; Kovalevsky, A. Y.; Morrow, J. R.; Richard, J. P. *J. Am. Chem. Soc.* **2003**, *125*, 1988–1993. (b) Iranzo, O.; Richard, J. P.; Morrow, J. R. *Inorg. Chem.* **2004**, *43*, 1743–1750. (c) Iranzo, O.; Elmer, T.; Richard, J. P.; Morrow, J. R. *Inorg. Chem.* **2003**, *42*, 7737–7746.

(44) (a) Yang, M.-Y.; Iranzo, O.; Richard, J. P.; Morrow, J. R. *J. Am. Chem. Soc.* **2005**, *127*, 1064–1065. (b) Yang, M.-Y.; Morrow, J. R.; Richard, J. P. *Bioorg. Chem.* **2007**, *35*, 366–374. (c) Yang, M.-Y.; Richard, J. P.; Morrow, J. R. *Chem. Commun.* **2003**, 2832–2833. (d) O'Donoghue, A.; Pyun, S. Y.; Yang, M.-Y.; Morrow, J. R.; Richard, J. P. *J. Am. Chem. Soc.* **2006**, *128*, 1615–1621.

(45) Fan, Y.; Gao, Y. Q. *Acta Phys.-Chim. Sin.* **2010**, *26*, 1034–1042.

(46) Fisch, M. J. et al. *Gaussian 03, Revision D.01*; Gaussian, Inc.: Wallingford, CT, 2004.

(47) Becke, A. D. *J. Chem. Phys.* **1993**, *98*, 5648–5652.

(48) Lee, C.; Yang, W.; Parr, R. G. *Phys. Rev. B* **1988**, *37*, 785–789.

(49) Dolg, M.; Wedig, U.; Stoll, H.; Preuss, H. *J. Chem. Phys.* **1987**, *86*, 866–872.

(50) (a) Reed, A. E.; Weinstock, R. B.; Weinhold, F. *J. Chem. Phys.* **1985**, *83*, 735–746. (b) Reed, A. E.; Curtiss, L. A.; Weinhold, F. *Chem. Rev.* **1988**, *88*, 899–926.

(51) NBO analysis was performed using the NBO Version 3.1, as implemented in the Gaussian 03 package by Glendening, E. D.; Badenhoop, J. K.; Reed, A. E.; Carpenter, J. E.; Weinhold, F.

(52) (a) Gonzalez, C.; Schlegel., H. B. *J. Phys. Chem.* **1990**, *94*, 5523–5527. (b) Gonzalez, C.; Schlegel., H. B. *J. Chem. Phys.* **1989**, *90*, 2154–2161.

(53) Cossi, M.; Scalmani, G.; Rega, N.; Barone, V. *J. Chem. Phys.* **2002**, *117*, 43–54.

(54) (a) Hengge, A. C. *Acc. Chem. Res.* **2002**, *35*, 105–112. (b) Zalatan, J. G.; Catrina, I.; Mitchell, R.; Grzyska, P. K.; O'Brien, P. J.; Herschlag, D.; Hengge, A. C. *J. Am. Chem. Soc.* **2007**, *129*, 9789–9798. (c) Hengge, A. C. *Adv. Phys. Org. Chem.* **2005**, *40*, 49–108.

(55) (a) Berti, P. J.; McCann, J. A. B. *Chem. Rev.* **2006**, *106*, 506–555. (b) McCann, J. A. B.; Berti, P. J. *J. Am. Chem. Soc.* **2008**, *130*, 5789–5797. (c) McCann, J. A. B.; Berti, P. J. *J. Am. Chem. Soc.* **2007**, *129*, 7055–7064.

(56) Liu, Y.; Lopez, X.; York, D. M. *Chem. Commun.* **2005**, 3909–3911.

(57) Becke, A. D. *J. Chem. Phys.* **1993**, *98*, 1372–1377.

(58) (a) Tao, J.; Perdew, J. P.; Staroverov, V. N.; Scuseria, G. E. *Phys. Rev. Lett.* **2003**, *91*, 146401. (b) Staroverov, V. N.; Scuseria, G. E.; Tao, J.; Perdew, J. P. *J. Chem. Phys.* **2003**, *119*, 12129–12137.

(59) The experimental activation free energy values approximately calculated from the observed rate constant (ref 44c), using the equation of $k = (k_bT/h)\exp(-\Delta^{\neq}G_m/RT)$, where k, k_b, h, R, T, $\Delta^{\neq}G_m$ are the rate constant, Boltzmann constant, Planck constant, universal gas constant, absolute temperature and active free energy in the standard state of a mole particles, respectively.

(60) (a) Bach, R. D.; Gonzales, C.; Andres, J. L.; Schlegel, H. B. *J. Org. Chem.* **1995**, *60*, 4653–4656. (b) Lewis, D. E.; Sims, L. B.; Yamataka, H.; McKenna, J. *J. Am. Chem. Soc.* **1980**, *102*, 7411–7419.

(61) (a) Scott, A. P.; Radom, L. *J. Phys. Chem.* **1996**, *100*, 16502–16513. (b) Wong, M. W. *Chem. Phys. Lett.* **1996**, *256*, 391–399. (c) Glad, S. S.; Jensen, F. *J. Phys. Chem.* **1996**, *100*, 16892–16898.

(62) (a) Hengge, A. C.; Cleland, W. W. *J. Am. Chem. Soc.* **1990**, *112*, 7421–7422. (b) Hengge, A. C.; Hess, R. A. *J. Am. Chem. Soc.* **1994**, *116*, 11256–11263.

(63) In the absence of catalyst, the EIEs (1.0245 and 1.0002) for deprotonation of **HpPNP** were calculated using the program ISOEFF98 with PCM/B3LYP/6-31+G(d,p) by Hengge and co-workers (ref 28). We also recalculated the EIEs at the level of PCM/B3LYP/6-31G(d,p) within the harmonic oscillator/rigid rotor approximations, as implemented in the Gaussian 03 program. Our results are similar to the values of ref 28.

(64) Hunt, H. R.; Taube, H. *J. Phys. Chem.* **1959**, *63*, 124–125.

(65) Sadlej-Sosnowska, N. *Theor. Chem. Acc.* **2007**, *118*, 281–293.

(66) Further improvement of various quantum theoretical techniques and developing a methodology is needed to accurately calculate the pK_a or the free energy change of for the deprotonation of a large molecule such as the dissociation reaction for HpPNP $\rightarrow$ $HpPNP^- + H^+$.

(67) (a) Velikyan, I.; Acharya, S.; Trifonova, A.; Földesi, A.; Chattopadhyaya, J. *J. Am. Chem. Soc.* **2001**, *123*, 2893–2894. (b) Lönnberg, H.; Strömberg, R.; Williams, A. *Org. Bimmol. Chem.* **2004**, *2*, 2165–2167.

(68) This free energy change value (ΔG) of the dissociation reaction (HpPNP $\rightarrow$ $HpPNP^- + H^+$) is approximately calculated by the formula $\Delta G = 2.303RT(pK_a)$, where R and T are the universal gas constant and absolute temperature, respectively. The experiment pK_a values (ref 67) are about 13, and in 298.15K, the rough free energy change values are approximately estimated to be about 17.7 kcal/mol.

(69) The sum of the bond orders to the nucleophile and leaving group is less than 1 in a loose transition state, while this sum is greater than 1 in a tight (or associative) transition state (see refs 54a and 54c for details).

(70) The orbital interaction energies are roughly estimated by the second order perturbation theory analysis of the Fock Matrix in a NBO basis.

(71) In Fan and Gao's work (ref 45), the TPSS density functional theory (with density fitting functions included) was employed. The basis set 6-31++G(d′,p′) was used for N, O, aromatic C, and all H atoms bound to N and O, while 6-31G was used for alkyl C and the rest of all H atoms, SDD was used for Zn atoms, and LANL2DZ plus a d-polarization, and a p-diffuse function was used for P atom.